Bioorganic & Medicinal Chemistry xxx (xxxx) xxx–xxx

Contents lists available at ScienceDirect

Bioorganic & Medicinal Chemistry

journal homepage: www.elsevier.com/locate/bmc

An SAR study of hydroxy-trifluoromethylpyrazolines as inhibitors of Orai1-mediated store operated Ca^{2+} entry in MDA-MB-231 breast cancer cells using a convenient Fluorescence Imaging Plate Reader assay

Ralph J. Stevenson[a,*], Iman Azimi[b,c,d], Jack U. Flanagan[a,e], Marco Inserra[f,g], Irina Vetter[f,g], Gregory R. Monteith[b,c], William A. Denny[a,e,*]

[a] Auckland Cancer Society Research Centre, School of Medical Sciences, The University of Auckland, Private Bag 92019, Auckland 1142, New Zealand
[b] The School of Pharmacy, The University of Queensland, Brisbane, Queensland, Australia
[c] Mater Research Institute, The University of Queensland, Translational Research Institute, Brisbane, Queensland, Australia
[d] Division of Pharmacy, College of Health and Medicine, University of Tasmania, Hobart, Tasmania, Australia
[e] Maurice Wilkins Centre for Molecular Biodiscovery, The University of Auckland, Private Bag 92019, Auckland 1142, New Zealand
[f] Institute for Molecular Bioscience, The University of Queensland, St Lucia, Queensland 4072, Australia
[g] School of Pharmacy, The University of Queensland, Woolloongabba, Queensland 4102, Australia

ARTICLE INFO

Keywords:
Orai1
Store-operated Ca^{2+} entry (SOCE)
Ca^{2+} release-activated Ca^{2+} (CRAC) channel
Triple negative breast cancer
Inhibitor
Hydroxy-trifluoromethylpyrazoline
Structure-activity relationship (SAR)

ABSTRACT

The proteins Orai1 and STIM1 control store-operated Ca^{2+} entry (SOCE) into cells. SOCE is important for migration, invasion and metastasis of MDA-MB-231 human triple negative breast cancer (TNBC) cells and has been proposed as a target for cancer drug discovery. Two hit compounds from a medium throughput screen, displayed encouraging inhibition of SOCE in MDA-MB-231 cells, as measured by a Fluorescence Imaging Plate Reader (FLIPR) Ca^{2+} assay. Following NMR spectroscopic analysis of these hits and reassignment of their structures as 5-hydroxy-5-trifluoromethylpyrazolines, a series of analogues was prepared via thermal condensation reactions between substituted acylhydrazones and trifluoromethyl 1,3-dicarbonyl arenes. Structure-activity relationship (SAR) studies showed that small lipophilic substituents at the 2- and 3-positions of the RHS and 2-, 3- and 4-postions of the LHS terminal benzene rings improved activity, resulting in a novel class of potent and selective inhibitors of SOCE.

1. Introduction

The Orai family (Orai1, Orai2 and Orai3) of proteins, first identified in 2006,[1–5] are plasma membrane proteins which share no homology with any other known calcium channel family. The Orai1 isoform is the key protein of the pore which forms the Ca^{2+} release-activated Ca^{2+} (CRAC) channel, which is activated upon depletion of endoplasmic reticulum (ER) Ca^{2+} stores. Reduced levels of ER Ca^{2+} are sensed by stromal interaction molecule 1 (STIM1 and its homologue STIM2), and prompt STIM1 to relocate and form puncta[6] near the plasma membrane. Protein-protein interactions with Orai1 then promote Ca^{2+} influx via the pathway referred to as store-operated Ca^{2+} entry (SOCE).[7] Elevation of intracellular Ca^{2+} rapidly induces dissociation of the Orai1/STIM1 complex, preventing Ca^{2+} overloading and may represent a SOCE gating mechanism.[8,9] Orai1 is involved in a number of physiological functions. Orai1-mediated Ca^{2+} influx plays a key role in the activation, differentiation and proliferation of T lymphocytes,[1,10] lactation,[11,12] cardiovascular/respiratory processes[13] and pancreatic cell function/dysfunction.[14] However, Orai1, its homologue Orai3 and activators STIM1 and STIM2 have also been implicated in tumor cell proliferation, invasion, survival, migration and therapy resistance in such cancers as prostrate, colorectal, melanoma, ovarian, cervical, leukemia, nasopharyngeal, pancreatic, lung, renal, glioblastoma, neuroblastoma, epidermoid, hepatoma and pertinent to the current study - breast cancer.[15–19] Elevated levels of Orai1 and alterations in the relative levels of STIM1/STIM2 are a feature of the poor prognosis of the basal breast cancer subtype.[12] It has been shown that blockage or knockdown of Orai1 or STIM1 reduces enolase-1 dependent migration of highly metastatic MDA-MB-231 triple negative basal-type breast cancer (TNBC)[20] cells, indicating a crucial role of SOCE in the

Abbreviations: FLIPR, Fluorescence Imaging Plate Reader; STIM1, stromal interaction molecule 1; ER, endoplasmic reticulum; TNBC, triple negative breast cancer; SAR, structure activity relationship; LHS, left hand side; RHS, right hand side; THF, tetrahydrofuran; *i*-PrOH, isopropanol

* Corresponding authors at: Auckland Cancer Society Research Centre, The University of Auckland, Private Bag 92019, Auckland 1142, New Zealand (R.J. Stevenson, W.A. Denny).
E-mail addresses: r.stevenson@auckland.ac.nz (R.J. Stevenson), b.denny@auckland.ac.nz (W.A. Denny).

https://doi.org/10.1016/j.bmc.2018.05.012
Received 29 March 2018; Received in revised form 1 May 2018; Accepted 8 May 2018

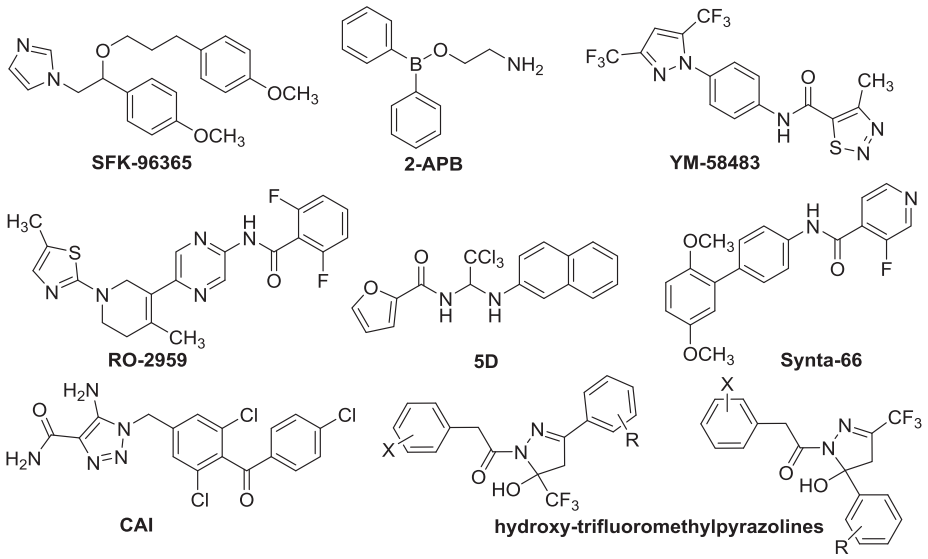

Fig. 1. Small molecule inhibitors of CRAC channels or SOCE reported in studies and new hydroxy-trifluoromethylpyrazolines.

modulation of cancer cell migratory and invasion properties.[21]

Orai1siRNA and STIM1 siRNA treatments or blockage of SOCE by a small molecule inhibitor (**SFK-96365**, Fig. 1) in a xenograft mouse model with MDA-MB-231 cells produced a significant antimetastatic effect indicating the potential for SOCE as a therapeutic target in breast cancer.[22] Whilst Orai1 and STIM1 are widely expressed, CRAC channel disorders appear to be limited with effects primarily in the immune system, skeletal muscle and ectodermal- derived tissue, providing a possible window of high selectivity and low toxicity for SOCE inhibitors.[23] With emerging evidence of SOCE implicated in a variety of diseases, the search and discovery of SOCE inhibitors is increasing and a variety of small molecule inhibitors have now been reported[19,24–26] opening the door for new therapeutic opportunities. Several small molecule SOCE inhibitors have shown promise in both *in vitro* and *in vivo* disease models (Fig. 1).

Although the aforementioned **SFK-96365** is not selective for CRAC channels with potential to block other Ca^{2+} channels,[27] it does block SOCE in mast,[26] rat basophilic leukemia,[28] Jurkat[29] and cervical cancer cells.[30] **2-APB** (Fig. 1), although also nonselective, inhibits the proliferation or migration of hepatoma,[31] cervical,[30] gastric[32] and colorectal cells.[33] **YM-58483** (Fig. 1) in one study appears to be relatively selective as it specifically inhibits SOCE and not other Ca^{2+} pathways in T lymphocytes with an IC_{50} of 10 nM against SOCE in Jurkat T cells.[34] It has also been shown to inhibit cytokine secretion in mast cells.[35] **RO-2959** (Fig. 1) is also thought to be relatively selective and has an IC_{50} of 400 nM against SOCE in rat basophilic leukemia-2H3 cells.[36] **5D** (Fig. 1) has been shown to inhibit CRAC channel activity by blocking ion permeation and diminishing the severity of experimental autoimmune encephalomyelitis in mice by inhibition of differentiation of inflammatory T cells.[37] The CRAC channel blocker **Synta-66** (Fig. 1) produced an IC_{50} of 1.4 μM in rat basophilic leukemia cells and Jurket T cells, with demonstrated good selectivity and an absence of activity against a range of other enzyme, receptor and ion channel targets.[38]

It has been demonstrated that Ca^{2+} is involved in a variety of cancer cell signalling pathways[39–41] and a recent review outlined the crucial role of Orai and STIM proteins in the hallmarks of cancer.[42] However, there are currently no CRAC channel inhibitors in the marketplace for treating cancer,[43] although carboxyamidotriazole **CAI** (Fig. 1) did reach a phase II clinical trial for patients with relapsed epithelial ovarian cancer.[44] **CM2489**, produced by CalciMedica with structure undisclosed and in phase I clinical trials for plaque psoriasis, is claimed to be the only specific CRAC channel inhibitor tested in patients.[45]

TNBC comprises 12–20% (of these ~75% are basal-type) of total breast cancers.[46] Patients with TNBC are characterised by absence of the estrogen receptor, the progesterone receptor and HER2 and have a poor prognosis compared to other subtypes.[46] Thus there is an urgent need for new selective targeted therapies for TNBC.[47,48] Recently we reported[49] the use of a Fluorescence Imaging Plate Reader (FLIPR) assay in the evaluation of 13 known compounds and a small series of novel iminotriazoles as selective SOCE inhibitors in MDA-MB-231 TNBC cells. We now outline the synthesis and an extensive structure–activity relationship (SAR) study of a series of hydroxy-trifluoromethylpyrazolines (Fig. 1) using this method.

2. Results and discussion

2.1. Chemistry

Although 1,3-diazoles and imidazoles are widely observed in natural products, the isomeric pyrazoles are somewhat rare.[50] Nevertheless, there are a number of manuscripts outlining the potential use of pyrazoles as pharmaceuticals: riboflavin synthase inhibitors,[51] COX-2 inhibitors,[52,53] sEH inhibitors,[54] HIV-1 reverse transcriptase inhibitors,[55] and NHE-1 inhibitors.[56] The thermal condensation of hydrazines and 1,3-dicarbonyls produces pyrazoles and in some cases, intermediate hydroxy-dihydropyrazolines can be isolated.[50,51,57] From a screen of 2140 purchased compounds,[49] 34 hydroxy-pyrazolines were tested. The regio-isomers **5648159** and **6068529**, based on the vendor's structures, were selected as hits as they displayed propitious inhibition of SOCE using the FLIPR assay in MDA-MB-231 cells (Fig. 2). However, the ^1H NMR ($CDCl_3$) spectra for both **5648159** and **6068529** were absolutely identical, so a detailed NMR spectroscopy study was undertaken in order to identify the correct structure. The diagnostic 5-OH proton appeared at δ 6.14 ppm. Previous mechanistic and synthetic

Fig. 2. Vendor's provided structures for **5648159** and **6068529**. ^1H, ^{13}C and ^{19}F NMR spectral analysis revealed that both compounds have the structure given for **6068529**.

studies by several groups[50,51,57] on the regioisomeric formation of hydroxy-pyrazolines from condensation of acylhydrazines and 1,3-diketones demonstrated that if the 5-OH proton was adjacent to a strong electron withdrawing group (EWG) (*e.g.* CF_3), there was a significant downfield shift (5-OH appearing at δ 6.59–6.87 ppm) compared with the OH moiety not adjacent to such a group (5-OH appearing at δ 5.20–5.58 ppm). Thus in the present case, the observed chemical shift supports **6068529**. In the ^{13}C NMR ($CDCl_3$) spectra, the observed signal from C5 was a quartet at δ 92.2 ppm (J_{CF} = 34.3 Hz) and the C3 atom gave a singlet at δ 153.3 ppm. This also supports **6068529** for if the structure was **5648159**, the signal for the sp^2-hybridised C3 atom would be a quartet with a significant downfield shift (δ 140–150 ppm)[51] from the value observed at 92.2 ppm, *i.e.* the CF_3 group is attached to an sp^3-hybridised carbon rather than the C=N carbon atom. In the ^{19}F NMR ($CDCl_3$) spectra, the signal at δ −6.02 ppm (CF_3) upfield from CF_3COOH (external standard) also supports **6068529** as the structure. It has been previously demonstrated that δ −4 to −3 ppm (CF_3) relative to CF_3COOH implies that a CF_3 moiety is attached to an sp^3-hybridised carbon atom.[51] If CF_3 is attached to an sp^2-hybridised carbon atom then δ > +10 ppm (CF_3) downfield from CF_3COOH would be observed.[51] It was concluded that both **5648159** and **6068529** had the given **6068529** structure (Fig. 2).

The new hydroxy-5-trifluoromethylpyrazolines and hydroxy-3-trifluoromethylpyrazolines were prepared by the thermal condensation[50,51,57] of 2-phenylacetohydrazide (**1**) or modified hydrazides (**44–46, 69**)[58] with phenyl- substituted 4,4,4-trifluoro-1-phenylbutane-1,3-diones (**3**) (Schemes 1–4), which in turn were prepared from substituted acetophenones (**2**) and ethyl trifluoroacetate in the presence of NaH (Scheme 1).[50–52,57,59] In the majority of reactions, the only regioisomer isolated was the one with a CF_3 moiety attached to an sp^3-hybridised carbon atom and hence geminal to an OH group (Tables 1–3). In our attempts to synthesis both hit compounds, only a compound (**14**) with ^1H NMR spectrum identical in all respects to **6068529** was isolated. However, in a few cases the alternative regioisomer where the CF_3 group is attached to an sp^2-hybridised carbon was either solely or also isolated (Table 4). The mechanism and regioselectivity of the condensation reaction between 1,3-diketones and hydrazines resulting in hydroxy-pyrazolines and pyrazoles has been previously studied.[50,51,57,60] It is well documented that in numerous instances, such reactions do not proceed with a defined regio-chemistry. In a number of examples, it was demonstrated that in reactions of acylhydrazones with 1,3-diketones F_3CCOCH_2COAr under neutral conditions, stable hydroxy-pyrazolines can be isolated.[50,51,57,60] Under acidic conditions or in the absence of a strong terminal EWG (*e.g.* CF_3), the reactions generally proceed to pyrazoles. Proposed partial mechanisms for the formation of regio-isomers hydroxy-5-trifluoromethylpyrazolines and hydroxy-3-trifluoromethylpyrazolines are outlined in Fig. 3. It has previously been discovered in such condensation reactions that aryl 1,3-diketones possessing a $COCF_3$ moiety exist predominantly as hemiketals due to nucleophilic addition of solvent,[61] in our examples *i*-PrOH (possibility A in Fig. 3). Formation of a trifluoromethylated hemiketal may explain why the majority of final products isolated were hydroxy-5-trifluoromethylpyrazolines (Schemes 1–3). However, the trifluoromethylated carbonyl group might be expected to be the more

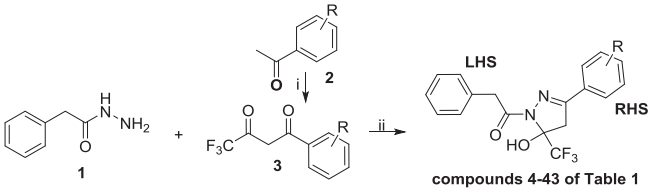

Scheme 1. Synthesis of the 5-hydroxy-5-trifluoromethylpyrazolines of Table 1. Reagents and conditions: (i) NaH/THF, then ethyl trifluoroacetate (0 °C to r.t. over 24 h); (ii) *i*-PrOH (90 °C over 48–96 h).

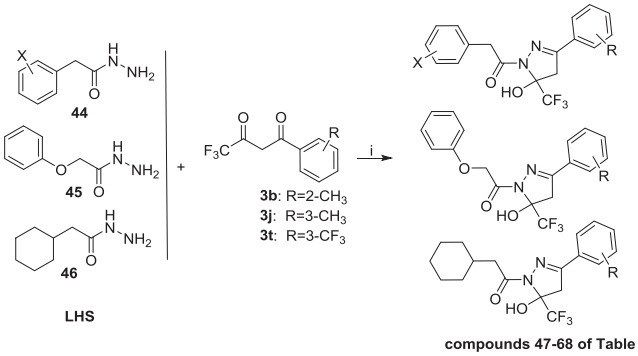

Scheme 2. Synthesis of the 5-hydroxy-5-trifluoromethylpyrazolines of Table 2. Reagents and conditions: (i) *i*-PrOH (90 °C over 48–96 h).

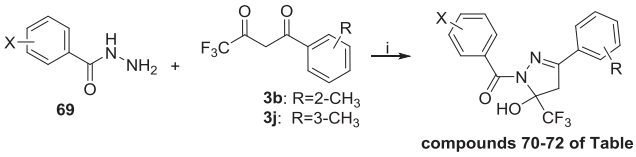

Scheme 3. Synthesis of the 5-hydroxy-5-trifluoromethylpyrazolines of Table 3. Reagents and conditions: (i) *i*-PrOH (90 °C over 48–96 h).

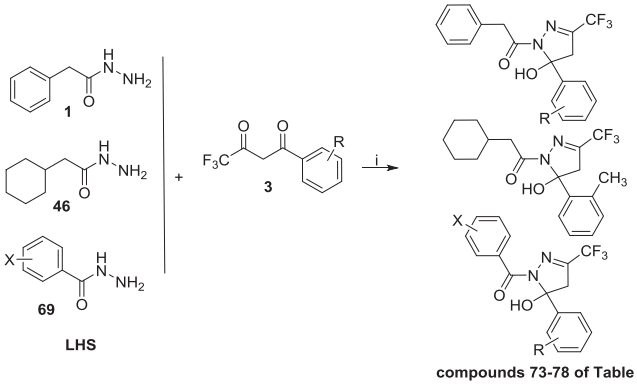

Scheme 4. Synthesis of the 5-hydroxy-3-trifluoromethylpyrazolines of Table 4. Reagents and conditions: (i) *i*-PrOH (90 °C over 48–96 h).

electrophilic and hence more reactive carbonyl group (possibility B in Fig. 3) due to the strongly electron withdrawing CF_3 moiety. This may explain why in some of our reactions, hydroxy-3-trifluoromethylpyrazolines were isolated (Scheme 4). Singh and co-workers[62] have noted that aryl trifluoromethyl-β-diketones exist substantially in the enol form providing an Ar−C=C−C=O extended conjugated system. Thus they have postulated that the first step is possibly conjugate addition of nitrogen onto the enol, eventually leading to the isolated products. It has previously been observed that in the crystalline state, products of possibility B exist entirely as hydroxy-3-trifluoromethylpyrazolines. However in $CDCl_3$, they exist as equilibrium mixtures of open hydrazones and cyclic tautomers[57] (possibility B in Fig. 3) and in a few ^1H NMR spectra of hydroxy-3-trifluoromethylpyrazolines, peaks appeared noticeably broader. Both possible covalently hydrated pyrazoles are stabilized by the electron withdrawing amide and CF_3 moieties. Hence, hydroxy-5-trifluoromethylpyrazolines and hydroxy-3-trifluoromethylpyrazolines can be isolated as stable entities.

In the present work, we first synthesised the hit compound (**14**) and then modified the RHS of the scaffold (Scheme 1, Table 1). The left hand side (LHS) was then modified whilst the RHS was kept relatively constant by retaining 2-CH_3 or 3-CH_3 moieties (Scheme 2, Table 2). The SAR was extended further by synthesising a series of pyrazolines where

Table 1
Yields and biological properties of 5-hydroxy-5-trifluoromethylpyrazolines.

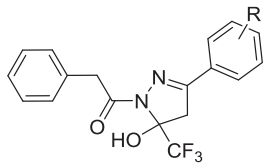

No	R	Yield %	IC_{50}[a] (μM) ER release (Peak 1)	IC_{50}[a] (CI) (μM) SOCE (Peak2)
4	H	71	na[b]	na[b]
5	2-CH_3	15	na[b]	50% at 30 μM[c]
6	2-OCH_3	14	na[b]	25% at 100 μM[c]
7	2-F	16	na[b]	30% at 100 μM[c]
8	2-Cl	33	50% at 100 μM[c]	33 (26–41)
9	2-Br	19	na[b]	30 (26–36)
10	2-OCF_3	37	na[b]	na[b]
11	2-NO_2	8	na[b]	40% at 100 μM[c]
12	2-aza	58	na[b]	20% at 100 μM[c]
13	3-CH_3	94	na[b]	36 (31–43)
14	3-OCH_3	48	na[b]	37% at 100 μM[c]
15	3-O$(CH_2)_2$W	57	50% at 100 μM[c]	50% at 100 μM[c]
16	3-F	92	na[b]	60% at 30 μM[c]
17	3-Cl	74	na[b]	48 (34–66)
18	3-Br	71	na[b]	47 (23–100)
19	3-OCF_3	97	na[b]	50% at 100 μM[c]
20	3-NO_2	92	na[b]	89 (55–142)
21	3-aza	88	na[b]	na[b]
22	3-CN	74	na[b]	na[b]
23	3-CF_3	82	na[b]	29 (24–35)
24	3-$NHSO_2CH_3$	36	na[b]	20% at 30 μM[c]
25	3-$NHCOCF_3$	82	na[b]	60% at 30 μM[c]
26	4-CH_3	69	na[b]	na[b]
27	4-OCH_3	10	na[b]	na[b]
28	4-F	31	na[b]	na[b]
29	4-Cl	69	na[b]	na[b]
30	4-Br	83	na[b]	na[b]
31	4-OCF_3	43	na[b]	na[b]
32	4-NO_2	55	na[b]	na[b]
33	4-aza	49	na[b]	na[b]
34	4-CN	70	na[b]	na[b]
35	4-$NHCOCH_3$	30	na[b]	na[b]
36	4-W	33	na[b]	na[b]
37	2,6-diOCH_3	68	na[b]	na[b]
38	2,3-diF	14	na[b]	80% at 100 μM[c]
39	2,6-diF	43	na[b]	na[b]
40	2,4-diCl	34	na[b]	58 (47–71)
41	2,5-diCl	45	na[b]	54 (44–66)
42	3,4-$(CH_2)_4$	47	na[b]	89 (62–129)
43	X	32	na[b]	na[b]

[a] IC_{50} is drug concentration for a half-maximal response.
[b] Less than 10% inhibition at 100 μM; na = not active.
[c] Estimate of activity where 100% inhibition not reached. CI = 95% Confidence Intervals (n = 4). W = morpholide, X = 2-thiophene.

the LHS had been modified producing phenylmethanones (Scheme 3, Table 3). Although we were unable to isolate a hydroxy-3-trifluoromethylpyrazoline corresponding to the structure for **5648159** (Fig. 2) assigned by the vendor, from some reactions we did isolate and characterise several hydroxy-3-trifluoromethylpyrazolines (Scheme 4, Table 4). Hydroxy-3-trifluoromethylpyrazolines were able to be distinguished from their regio-isomeric hydroxy-5-trifluoromethylpyrazolines by the diagnostic ^{1}H NMR 5-OH proton signal appearing upfield at δ 4.95–5.30 ppm. In fact, in the reaction of **1** with **3** containing a 2-CF_3 substituted phenyl group the only product isolated was a hydroxy-3-trifluoromethylpyrazoline (**73**) (Scheme 4, Table 4). The major product of the reaction of **1** with **3** containing a 2-NO_2 substituted phenyl group was a hydroxy-3-trifluoromethylpyrazoline (**74**) (Scheme 4, Table 4). Strikingly, hydroxy-3-trifluoromethylpyrazoline **78** (3-CH_3, RHS; 2-I, LHS) was produced in

Table 2
Yields and biological properties of 5-hydroxy-5-trifluoromethylpyrazolines; LHS modifications.

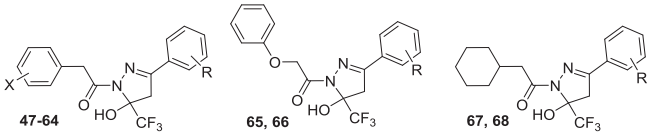

No	X or LHS	R	Yield %	IC_{50}[a] (μM) ER release (Peak 1)	IC_{50}[a] (CI) (μM) SOCE (Peak2)
47	2-OCH_3	2-CH_3	12	na[b]	60% at 100 μM[c]
48	2-OCH_3	3-CH_3	32	na[b]	50% at 100 μM[c]
49	3-OCH_3	2-CH_3	7	na[b]	60% at 100 μM[c]
50	3-OCH_3	3-CH_3	48	na[b]	32 (24–43)
51	4-OCH_3	2-CH_3	30	na[b]	30% at 100 μM[c]
52	4-OCH_3	3-CH_3	16	na[b]	33 (30–37)
53	2-CH_3	2-CH_3	28	na[b]	20% at 100 μM[c]
54	2-CH_3	3-CH_3	50	na[b]	na[b]
55	3-CH_3	2-CH_3	14	na[b]	42 (32–55)
56	3-CH_3	3-CH_3	72	na[b]	45 (38–54)
57	4-CH_3	2-CH_3	20	na[b]	55 (43–71)
58	4-CH_3	3-CH_3	50	na[b]	42 (32–54)
59	2-Cl	2-CH_3	49	na[b]	40 (35–45)
60	2-Cl	3-CH_3	73	na[b]	42 (35–50)
61	3-Cl	2-CH_3	19	na[b]	79 (69–91)
62	3-Cl	3-CH_3	49	na[b]	75 (64–88)
63	4-Cl	2-CH_3	44	na[b]	47 (38–59)
64	4-Cl	3-CH_3	63	na[b]	60 (40–91)
65	**45**	2-CH_3	18	na[b]	105 (74–149)
66	**45**	3-CH_3	50	na[b]	na[b]
67	**46**	2-CH_3	28	na[b]	na[b]
68	**46**	3-CH_3	57	na[b]	na[b]

[a] IC_{50} is drug concentration for a half-maximal response.
[b] Less than 10% inhibition at 100 μM; na = not active.
[c] Estimate of activity where 100% inhibition not reached. CI = 95% Confidence Intervals (n = 4).

Table 3
Yields and biological properties of 5-hydroxy-5-trifluoromethylpyrazolines; LHS modifications.

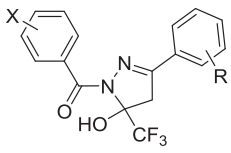

No	X	R	Yield %	IC_{50}[a] (μM) ER release (Peak 1)	IC_{50}[a] (μM) SOCE (Peak2)
70	H	2-CH_3	18	na[b]	20% at 100 μM[c]
71	H	3-CH_3	37	na[b]	30% at 100 μM[c]
72	2-I	3-CH_3	17	nt[d]	nt[d]

[a] IC_{50} is drug concentration for a half-maximal response.
[b] Less than 10% inhibition at 100 μM; na = not active.
[c] Estimate of activity where 100% inhibition not reached.
[d] nt = not tested.

64% yield versus 17% for the 5-isomer **72**.

Overall, the yields of products varied from 7 to 97% (Tables 1–4), and appeared to be influenced by the nature and regio-chemistry of the aryl substituents at both ends of the pyrazolines. None of the reactions involving 2-substituted phenyl groups on the RHS provided high yielding products. This may be a steric hindrance issue as a number of products containing both 3-substituted and 4-substituted phenyl groups were isolated in high yield. Most notably, lower yields could sometimes be attributed to thermally-promoted dehydration reactions producing

Table 4
Yields and biological properties of 5-hydroxy-3-trifluoromethylpyrazolines; alternative isomers.

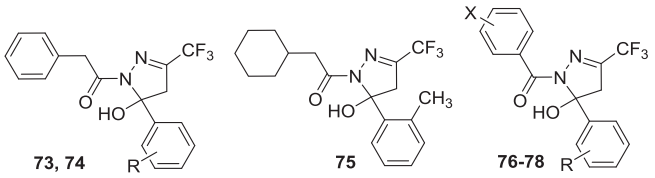

No	LHS	R	Yield%	IC_{50}[a] (CI) (μM) ER release (Peak 1)	IC_{50}[a] (CI) (μM) SOCE (Peak2)
73	**1**	2-CF_3	34	80 (59–108)	49 (40–60)
74	**1**	2-NO_2	40	20% at 100 μM[c]	30% at 100 μM[c]
75	**46**	2-CH_3	25	na[b]	20% at 100 μM[c]
76	**69** (X = H)	2-CH_3	10	na[b]	20% at 10 μM[c]
77	**69** (X = H)	3-CH_3	18	na[b]	na[b]
78	**69** (X = 2-I)	3-CH_3	64	nt[d]	nt[d]

[a] IC_{50} is drug concentration for a half-maximal response.
[b] Less than 10% inhibition at 100 μM; na = not active.
[c] Estimate of activity where 100% inhibition not reached. CI = 95% Confidence Intervals (n = 4).
[d] nt = not tested.

aromatic pyrazoles which rapidly lose the LHS acyl groups, due to the pyrazole moiety being a powerful leaving group in the presence of the nucleophilic solvent (*i*-PrOH).[63]

2.2. Biology and structure-activity relationships

The FLIPR Ca^{2+} assay is a convenient procedure for measuring intracellular free Ca^{2+} and we have previously validated this assay for assessment of Orai1-mediated Ca^{2+} influx in MDA-MB-231 cells.[12,49] The detailed procedure is described in the experimental section. In brief, addition of the sarco/endoplasmic reticulum ATPase (SERCA) inhibitor cyclopiazonic acid (CPA) induced a gradual loss of Ca^{2+} from internal stores and we designated this as peak 1 (red) in the normalised 2-peak FLIPR plots (% inhibition *vs* $\log_{10}$[M]). Ideally peak 1 should remain flat with increasing concentration of introduced compounds implying such compounds do not have pronounced non-specific direct effects on ER Ca^{2+} channels. The "2-peak assessment" allowed us to promptly identify analogues that were clearly not SOCE selective by observing if there was appreciable potency against peak 1.[51] Store depletion was promoted by selective chelation of extracellular Ca^{2+} with 1,2-bis(2-aminophenoxy)ethane-N,N,N′,N′-tetraacetic acid) (BAPTA). Addition of extracellular Ca^{2+} resulted in SOCE which we designated as peak 2 (black). A potent and selective SOCE inhibitor would cause peak 2 to reach 100% inhibition at a low concentration whilst peak 1 would remain flat in the 2-peak plots. We have previously demonstrated that peak 2 is reduced by silencing of Orai1 but not the related isoforms Orai2 and Orai3.[12,49]

The purchased hit compound **5648159** provided an estimated 37% inhibition of SOCE at 100 μM in MDA-MB-231 cells as indicated in peak 2 (Fig. 2) and importantly it was selective as peak 1 remained unchanged. Having the same structure (3-OCH_3, RHS), the purchased **6068529** (Fig. 2) and synthesised **14** gave identical 2-peak plots (Table 1). A variety of related structures were also evaluated. If a potential inhibitor did not reach 80–100% in either peak 1 or peak 2 an IC_{50} was not assigned for either peak 1 or peak 2 and if a compound showed less than 10% inhibition at 100 μM (even if it exhibited activity above 100 μM) it was designated as inactive against the relevant peak. Compound **14** did not reach the threshold in peak 2 and was therefore not allocated an IC_{50}.

Several of the thirteen 3-substituted aryl (RHS) synthesised analogues inhibited SOCE (peak 2) without non-specific effects on peak 1 (Table 1). Most notably, compound **23** (3-CF_3, RHS) provided an IC_{50} of 29 μM and 100% inhibition at 100 μM against peak 2 and was inactive against peak 1 (Figs. 4 and S1). Two 3-substituted halides, compound **17** (3-Cl, RHS) and compound **18** (3-Br, RHS) were both selective and active against SOCE providing IC_{50}s of 48 and 47 μM respectively and 100% inhibition at 100 μM against peak 2 and were inactive against peak 1 (Figs. 4 and S1). Compound **13** (3-CH_3, RHS) was also active against SOCE (IC_{50} 36, 100% inhibition at 100 μM against peak 2) but

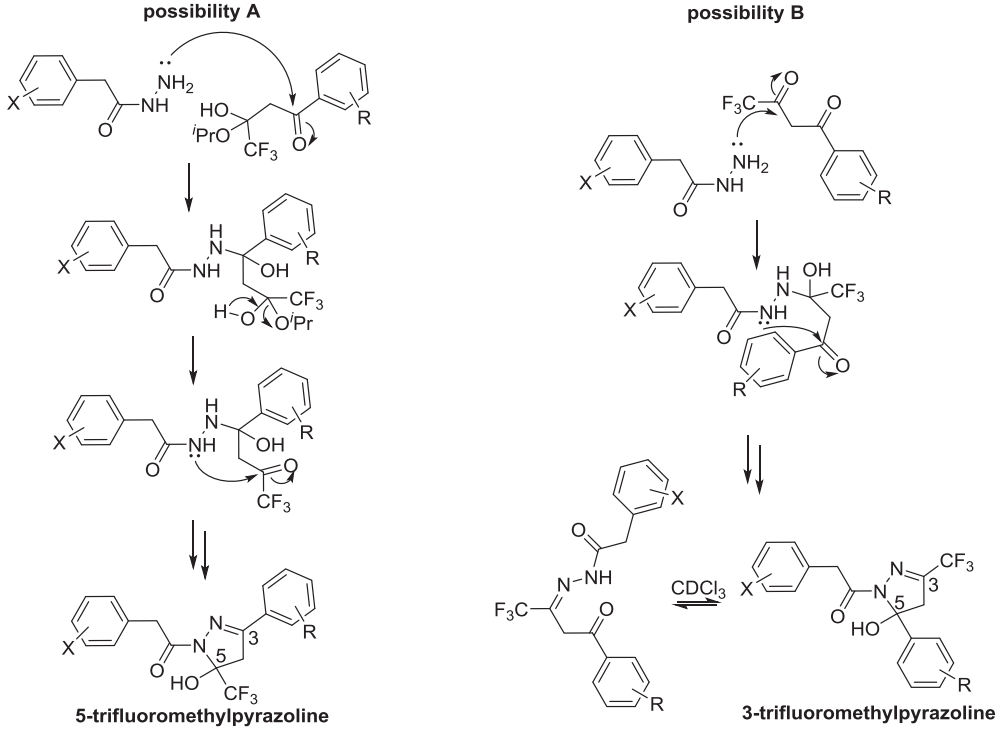

Fig. 3. Proposed partial mechanisms for formation of two possible hydroxy-trifluoromethylpyrazoline regio-isomers.

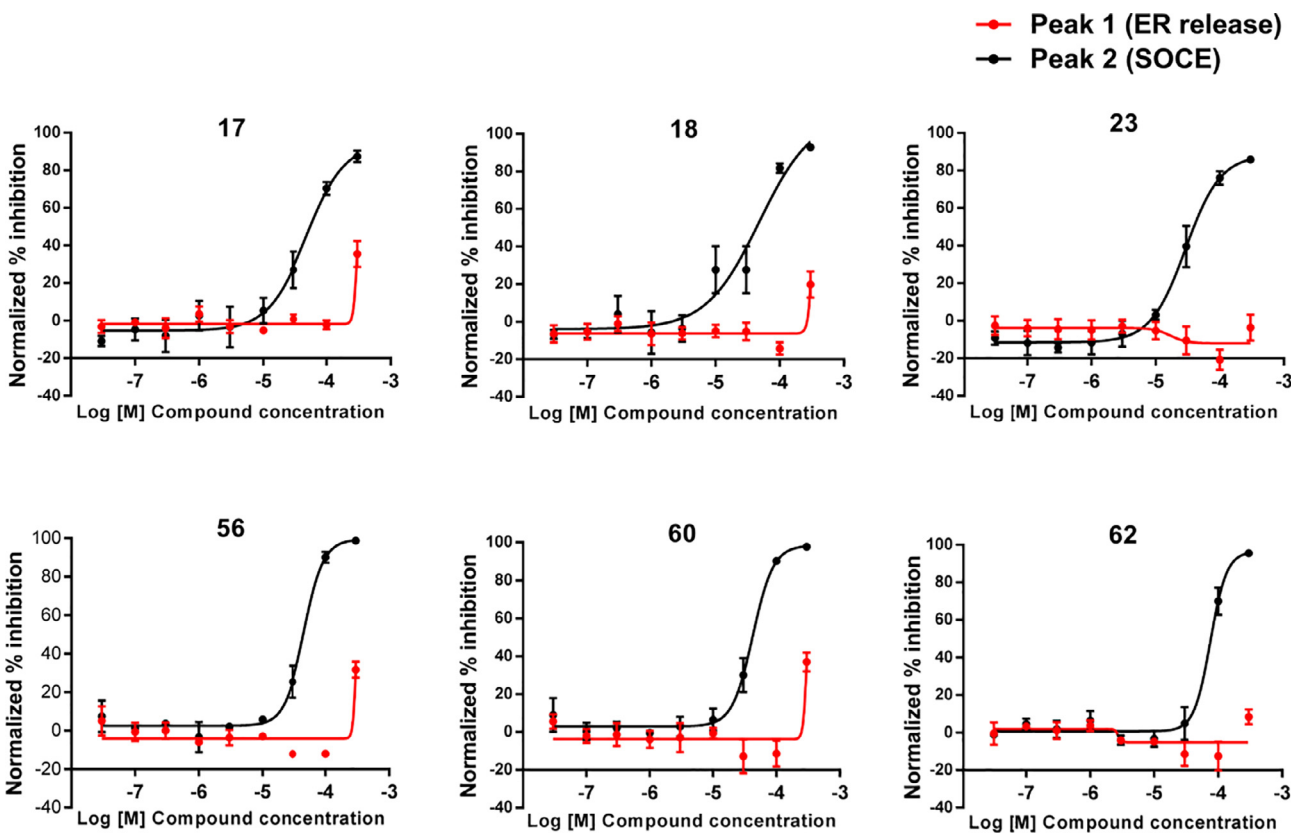

Fig. 4. Normalised FLIPR plots of compounds **17**, **18**, **23**, **56**, **60** and **62** demonstrating SOCE inhibition (black) and selectivity against ER release (red). (For interpretation of the references to colour in this figure legend, the reader is referred to the web version of this article.)

with some inhibition of peak 1 at 100 μM. Compounds **16** (3-F, RHS), **19** (3-OCF_3, RHS), **20** (3-NO_2, RHS) and **25** (3-$NHCOCF_3$, RHS) showed ~ 60% inhibition selectively at 100 μM against peak 2. Compound **15** (3-$O(CH_2)_2$morph, RHS) also provided 60% inhibition at 100 μM against peak 2 but was not selective.

Amongst the eight 2-substituted aryl (RHS) synthesised analogues, compounds **5** (2-CH_3, RHS) and **9** (2-Br, RHS) were the most selectively potent showing ~ 60% inhibition at 100 μM against peak 2. Compound **8** (2-Cl, RHS) showed 80% inhibition at 100 μM against peak 2 but was clearly not selective. Compounds **6** (2-OCH_3, RHS), **7** (2-F, RHS) and **11** (2-NO_2, RHS) provided ~25% inhibition selectively at 100 μM against peak 2.

None of the eleven 4-substituted aryl (RHS) compounds demonstrated any significant SOCE inhibition (Table 1). The best were compounds **33** (4-aza, RHS) and **36** (4-morph, RHS) showing 50% selective SOCE inhibition at 300 μM but overall their activity was poor. Since lack of activity is not due to Log *P* or solubility (Table S1), we postulate that steric bulk of 4-substituents may be the cause: 4-substitution is not well tolerated for SOCE inhibition unlike 2- and 3-substitutions where activity is improved.

The outcomes of the 7 di-substituted and miscellaneous (RHS) were more promising (Table 1). Compounds **38** (2,3-diF, RHS), **40** (2,4-diCl, RHS) and **41** (2,5-diCl, RHS) all provided IC_{50}'s of ~55 μM and ~60% inhibition at100 μM against peak 2. Compound **42** (3,4-$(CH_2)_4$, RHS) provided and an IC_{50} of 89 μM and 50% inhibition at100 μM selectively against peak 1.

Modification of the LHS (Table 2) proved fruitful as 12 of the 22 compounds synthesised provided > 80% inhibition of SOCE as evidenced by peak 2 in the FLIPR plots. Compounds **61** (2-CH_3, RHS; 3-Cl, LHS) and **62** (3-CH_3, RHS; 3-Cl, LHS, Fig. 4) demonstrated good selectivity and IC_{50}'s of 79 μM and 75 μM respectively. Compounds **50** (3-CH_3, RHS; 3-OCH_3, LHS), **52** (3-CH_3, RHS; 4-OCH_3, LHS), **55** (2-CH_3, RHS; 2-CH_3, LHS), **56** (3-CH_3, RHS; 3-CH_3, LHS, Fig. 4), **57** (2-CH_3, RHS; 4-CH_3, LHS), **58** (3-CH_3, RHS; 4-CH_3, LHS), **59** (2-CH_3, RHS; 2-Cl, LHS), **60** (3-CH_3, RHS; 3-Cl, LHS, Fig. 4), **63** (2-CH_3, RHS; 4-Cl, LHS) and **64** (3-CH_3, RHS; 4-Cl, LHS) all provided respectable IC_{50}'s (33–60 μM) although some were less selective at higher concentrations (Table 2).

None of the compounds listed in Table 3 (**70–72**) or Table 4 (**73–78**) appeared to be particularly effective SOCE inhibitors in the FLIPR assay.

The original hit compound **5648159** was also screened in the FLIPR assay for its ability to inhibit the TRPV1, TRPM8, $Ca_V1.2$/ $Ca_V1.3$ (*L*-type) and $Ca_V2.2$ (*N*-type) calcium channels. This compound showed no activity up to 100 μM against these channels, implying some selectivity for SOCE inhibition. **5648159** exhibited low inhibition of hERG (9.1% at 10 μM), $T_{1/2}$ (min) 8.2 in human liver microsomes, $T_{1/2}$ (min) 3.3 in mouse liver microsomes, a solubility of M(aMEM) = 16.8 μg/mL, a stability of M1/M0 (H_2O) = 93.2% and log *P* = 4.4.

2.3. Conclusions

With an urgent need for new selective targeted therapies for TNBC and the potential use of SOCE inhibitors in a variety of diseases, the discovery of a number of new active and potentially selective SOCE inhibitors (*e.g.* **18**, **23**, **60** and **63**) using our FLIPR Ca^{2+} assay in MDA-MB-231 cells is significant. Seizing on hits from a medium throughput screen and using a relatively simple synthetic strategy, we were able to observe SAR on a series of hydroxy-5-trifluoromethylpyrazolines and evaluate them for SOCE inhibition with the convenient FLIPR assay. Regarding the RHS of the hydroxy-5-trifluoromethylpyrazoline scaffold, it was clear that 2- (*e.g.* **9**) and 3-substitutions (*e.g.* **18**) on the aryl moiety provided superior activity/selectivity. Modifying the LHS proved profitable with activity/selectivity maintained with a variety of

substitutions round the aryl ring (*e.g.* **56**, **60** and **63**). Future studies will involve expanding the SAR and selection of the most active/selective analogues for patch-clamping studies (I_{CRAC}) and *in vivo* evaluations in tumor-containing mouse models. Given that the potency of **YM-58483** on inhibition of SOCE is greatly increased by extending the period of pre-incubation,[34] the effect of increased pre-incubation and also the reversibility of the SOCE inhibitors developed here should be assessed in future studies.

3. Experimental

3.1. Chemistry

Final products were analysed by reverse-phase HPLC (Alltima C18 5 μm column, 150 × 3.2 mm; Alltech Associated, Inc., Deerfield, IL) using an Agilent HP1100 equipped with a diode-array detector. Mobile phases were gradients of 80% CH_3CN/20% H_2O (v/v) in 45 mM NH_4HCO_2 at pH 3.5 and 0.5 mL/min. Purity was determined by monitoring at 330 ± 50 nm and was ≥95% for all final products. Combustion analyses were carried out in the Campbell Microanalytical Laboratory, University of Otago, Dunedin, New Zealand. High resolution mass spectra (HRMS) were measured on an Agilent Technologies 6530 Accurate-Mass Quadrupole Time of Flight (Q-TOF) LCMS interfaced with an Agilent Jet Stream Electrospray Ionization (ESI) source allowing positive or negative ions detection. Melting points were determined on an Electrothermal 2300 melting point apparatus. NMR spectra were obtained on a Bruker Avance 400 spectrometer at 400 MHz for ^{1}H and 100 MHz for ^{13}C spectra. The ^{19}F chemical shifts were reported relative to CF_3COOH (external standard).

General method for the synthesis of hydroxy-trifluoromethylpyrazolines (chemical data for all compounds are located in Supporting Information).

3.1.1. 1-(5-Hydroxy-3-phenyl-5-(trifluoromethyl)-4,5-dihydro-1H-pyrazol-1-yl)-2-phenylethan-1-one (4)

A mixture of 2-phenylacetohydrazide (**1**) (0.10 g, 0.67 mmol) and 1,1,1-trifluoro-5-phenylpentane-2,4-dione (**3a**) (0.14 g, 0.67 mmol) in a solution of *i*-PrOH (5 mL) was heated at 90 °C for 48 h. After cooling to room temperature, EtOAc and water were added. The EtOAc extract was washed with water, brine and dried (Na_2SO_4). Flash chromatography (petroleum ether/EtOAc; 100:0 to 93:7) followed by recrystallization from Et_2O/petroleum ether gave **4** (0.17 g, 71%), mp 122–123 °C (Et_2O/petroleum ether); ^{1}H NMR ($CDCl_3$) δ 7.74–7.69 (m, 2H), 7.52–7.43 (m, 3H), 7.37–7.31 (m, 4H), 7.29–7.24 (m, 1H), 6.16 (s, 1H), 4.17 (d, J = 14.9 Hz, 1H), 4.11 (d, J = 14.9 Hz, 1H), 3.68 (d, J = 18.6 Hz, 1H), 3.53 (dd, J = 18.6, 1.3 Hz, 1H). Anal. calcd. for $C_{18}H_{15}F_3N_2O_2$: C, 60.07; H, 4.34; N, 8.04. Found: C, 61.82; H, 4.34; N, 8.02.

3.2. Biology

3.2.1. Compound library development

A ligand based virtual screening approach used in two phases for the discovery of SOCE inhibitors was previously described.[49,64]

3.2.2. Measurement of intracellular free Ca^{2+} by FLIPR assay

MDA-MB-231 TNBC cells were plated at a density of 2 × 10^3 cells per well in 384-well black plates (Corning Costar, *Cambridge, MA, USA).* Three days post seeding, intracellular free Ca^{2+} levels were measured in a fluorescence imaging plate reader (FLIPR^{TETRA}, Molecular Devices, Sunnyvale, CA, USA) using the PBX Calcium Assay Kit (640175, BD Biosciences, Franklin Lakes, NJ, USA) as described previously.[65] Briefly, cells were first loaded for 1 h at 37 °C with a dye-loading solution comprising of 2 μM PBX Calcium Assay dye, 5% (v/v) PBX Signal Enhancer and 500 μM probenecid in physiological salt solution (PSS, 5.9 mM KCl, 1.4 mM $MgCl_2$, 10 mM HEPES, 1.2 mM NaH_2PO_4, 5 mM $NaHCO_3$, 140 mM NaCl, 11.5 mM glucose, pH 7.3). Cells were then treated for 15 min at room temperature with different concentrations of compound in a solution containing 5% (v/v) PBX Signal Enhancer and 500 μM probenecid in PSS. For assessment of store-operated Ca^{2+} entry (SOCE), which has been previously shown to be mediated by Orai1 proteins in MDA-MB-231 cells,[66] the following solutions in PSS were added in order inside the FLIPR^{TETRA} using a robotic arm: 500 μM BAPTA (Invitrogen, Carlsbad, CA, USA) for chelation of extracellular Ca^{2+}; 10 μM cyclopiazonic acid (CPA; Sigma-Aldrich, St Louis, MO) for inhibition of sarco/endoplasmic reticulum Ca^{2+}-ATPases (SERCA) pump and depletion of endoplasmic reticulum (ER);[67] 0.5 mM $CaCl_2$ (700 s after the addition of CPA) for assessment of store-operated Ca^{2+} influx. Fluorescence was measured at 470–495 nm excitation and 515–575 nm emission. ScreenWorks Software (v2.0.0.27, Molecular Devices) was used for data analyses. Ca^{2+} levels were assessed through the change in relative fluorescence of the Ca^{2+} dye. The percentage inhibition of the maximum peak height for each concentration of each compound normalized to its corresponding DMSO control was calculated and plotted separately for peak 1 (a measure of the release of endoplasmic reticulum calcium store) by addition of CPA to assess potential non-specific effects on Ca^{2+} homeostasis and peak 2 (a measure of store-operated Ca^{2+} influx).[26,68] Where the% inhibition of peak 2 (SOCE) did not exceed 10% at 100 μM in initial assessments, these compounds were defined as not active.

3.2.3. Selectivity screen

TRPV1 and TRPM8 responses were assessed in HEK293 cells (American Tissue Culture Collection, Manassas, VA, USA) 48 h after transfection with plasmid DNA of rTRPV1 (D. Julius, Department of Physiology, University of California, Berkeley, CA, USA) or rTRPM8 (P. Reeh, Department of Anesthesiology, Friedrich-Alexander-University, Erlangen-Nuremberg, Erlangen, Germany) using Lipofectamine 2000 as previously described.[69] $Ca_V2.2$ responses were assessed in SH-SY5Y neuroblastoma cells in the presence of nifedipine (10 μM) according to established protocols.[70] HEK293 cells were routinely maintained in DMEM containing 10% foetal bovine serum, 2 mM l-glutamine, pyridoxine and 110 mg/ml sodium pyruvate. SH-SY5Y cells (European Collection of Authenticated Cell Cultures, Salisbury, UK) were cultured in RPMI 1640 antibiotic-free medium (Invitrogen) supplemented with 15% heat-inactivated FBS and 2 mM GlutaMAX™ (Invitrogen). Cells were split every 3–6 days in a ratio of 1:5 using 0.25% trypsin/EDTA. Cells were plated on 384-well black-walled imaging plates (Corning) at a density of 10,000 cells/well (HEK293) or 50,000 cells/well (SH-SY5Y) and used for Ca^{2+} experiments 48 h after plating. Growth media was removed and replaced with 20 μl/well Calcium 4 No-Wash dye diluted according to the manufacturer's instructions in physiological salt solution (PSS; NaCl 140 mM, glucose 11.5 mM, KCl 5.9 mM, $MgCl_2$ 1.4 mM, NaH_2PO_4 1.2 mM, $NaHCO_3$ 5 mM, $CaCl_2$ 1.8 mM, HEPES 10 mM) and incubated for 30 min at 37 °C/5% CO_2. Ca^{2+} responses were measured using a FLIPR^{TETRA} (Molecular Devices, Sunnyvale, CA, USA) fluorescent plate reader with excitation at 470–495 nM and emission at 515–575 nM. Camera gain and intensity were adjusted for each plate to yield a minimum of 1500–2000 arbitrary fluorescence units (AFU) baseline fluorescence. Test compounds were added 300 s prior to stimulation with capsaicin (100 nM; TRPV1), menthol (100 μM, TRPM8) and KCl (90 mM)/$CaCl_2$ (5 mM; $Ca_V2.2$). Data was analysed using Screenworks 3.2 and FLIPR^{TETRA} data was plotted using GraphPad Prism™ software (Version 6.00).

Acknowledgements

The authors gratefully acknowledge funding from QUE Oncology Inc and the University of Auckland Biopharma Initiative. This work was supported by an Australian Research Council Future Fellowship FT130101215 awarded to I.V. We thank Karin Tan and Sisira Kumara for HPLC analysis.

Conflict of interests

G.R.M and W.A.D are associated with QUE Oncology Inc.

Supplementary data

Supplementary data associated with this article can be found, in the online version, at http://dx.doi.org/10.1016/j.bmc.2018.05.012.

References

1. Feske S, Gwack Y, Prakriya M, et al. *Nature.* 2006;441:179.
2. Vig M, Peinelt C, Beck A, et al. *Science.* 2006;312:1220.
3. Taylor CW. *Trends Biochem Sci.* 2006;31:597.
4. Zhang SL, Yeromin AV, Zhang XH, et al. *Proc Natl Acad Sci USA.* 2006;103:9357.
5. Yeromin AV, Zhang SL, Jiang W, Yu Y, Safrina O, Cahalan MD. *Nature.* 2006;443:226.
6. Zhang SL, Yu Y, Roos J, et al. *Nature.* 2005;437:902.
7. Luik RM, Wu MM, Buchanan J, Lewis RS. *J Cell Biol.* 2006;174:815.
8. Palty R, Isacoff EY. *J Biol Chem.* 2016;291:334.
9. Shim AH-R, Tirado-Lee L, Prakriya M. *J Mol Biol.* 2015;427:77.
10. Vaeth M, Yang J, Yamashita M, et al. *Nature Commun.* 2017. http://dx.doi.org/10.1038/ncomms14714.
11. Davis FM, Janoshazi A, Janardhan KS, et al. *Proc Natl Acad Sci USA.* 2015;112:5827.
12. McAndrew D, Grice DM, Peters AA, et al. *Mol Cancer Ther.* 2011;10:448.
13. Spinelli AM, Trebak M. *Am J Physiol-Cell Ph.* 2016;310:C402.
14. Son A, Park S, Shin DM, Muallem S. *Am J Physiol-Cell Ph.* 2016;310:C414.
15. Vashisht A, Trebak M, Motiani RK. *Am J Physiol-Cell Ph.* 2015;309:C457.
16. Chen Y-F, Hsu K-F, Shen M-R. *Biochim Biophys Acta.* 2016;1863:1427.
17. Jardin I, Rosado JA. *Biochim Biophys Acta.* 2016;1863:1418.
18. Hoth M. *Biochim Biophys Acta.* 2016;1863:1408.
19. Xie J, Pan H, Yao J, Zhou Y, Han W. *In J Cancer.* 2016;138:2067.
20. Chavez KJ, Garimella SV, Lipkowitz S. *Breast Dis.* 2010;32:35.
21. Didiasova M, Zakrzewicz D, Magdolen V, et al. *J Biol Chem.* 2015;290:11983.
22. Yang S, Zhang JJ, Huang X-Y. *Cancer Cell.* 2009;15:124.
23. Hogan PC, Lewis RS, Rao A. *Annu Rev Immunol.* 2010;28:491.
24. Putney JW. *Mol Interv.* 2010;10:209.
25. Sweeney ZK, Minatti A, Button DC, Patrick S. *ChemMedChem.* 2009;4:707.
26. Zhang H-Z, Xu X-I, Chen H-Y, et al. *Acta Pharmacol Sin.* 2015;36:1137.
27. Franzius D, Hoth M, Penner R. *Pflugers Arch.* 1994;428:433.
28. Kozak JA, Kerschbaum HH, Cahalan MD. *J Gen Physiol.* 2002;120:221.
29. Chung SC, McDonald TV, Gardner P. *Br J Pharmacol.* 1994;113:861.
30. Chen YF, Chiu WT, Chen YT. *Proc Natl Acad Sci USA.* 2011;108:15225.
31. Enfissi A, Prigent S, Colosetti P, et al. *Cell Calcium.* 2004;36:459.
32. Sakakura C, Miyagawa K, Fukuda K, et al. *Gan Kagaku Ryoho.* 2003;30:1784.
33. Wang JY, Sun J, Huang MY, et al. *Oncogene.* 2015;34:4358.
34. Zitt C, Strauss B, Schwarz EC, et al. *J Biol Chem.* 2004;279:12427.
35. Law M, Morales JL, Mottram LF, et al. *Int J Biochem Cell Biol.* 2011;43:1228.
36. Chen G, Panicker S, Lau K-Y, et al. *Mol Immunol.* 2013;54:355.
37. Kim KD, Srikanth S, Tan YV, et al. *J Immunol.* 2014;192:110.
38. Di Sabatino A, Rovedatti L, Kaur R, et al. *J Immunol.* 2009;183:3454.
39. Monteith GR, McAndrew D, Faddy HM, Roberts-Thomson SJ. *Nat Rev Cancer.* 2007;7:519.
40. Prevaskaya N, Skryma R, Shuba Y. *Nat Rev Cancer.* 2011;11:609.
41. Monteith GR, Davis FM, Roberts-Thomson SJ. *J Biol Chem.* 2012;287:31666.
42. Fiorio Pla A, Kondratska K, Prevaskaya N. *Am J Physiol-Cell Ph.* 2016;310:C509.
43. Tian C, Du L, Zhou Y, Li M. Future. *Med Chem.* 2016;8:817.
44. Hussain MM, Kotz H, Minasian L, et al. *J Clin Oncol.* 2003;21:4356.
45. Peverello P, Cainarca S, Liberati C, Tarroni P, Piscitelli F, Severi E. *Pharm Pat Anal.* 2014;3:171.
46. Anders CK, Carey LA. *Clin Breast Cancer.* 2009;9:S73.
47. Crown J, O'Shaughnessy J, Gullo G. *Ann Oncol.* 2012;23:6.
48. Wahba HA, El-Hadaad HA. Cancer. *Biol Med.* 2015;12:106.
49. Azimi I, Flanagan JU, Stevenson RJ, et al. *Bioorg Med Chem.* 2017;25:440.
50. Norris T, Colon-Cruz R, Ripin DHB. *Org Biomol Chem.* 2005;3:1884.
51. Zhao Y, Bacher A, Illarionov B, et al. *J Org Chem.* 2009;74:5297.
52. Gao M, Wang M, Miller KD, Zheng Q-H. *Euro J Med Chem.* 2011;46:4760.
53. Lin J, Lundy deMello KM, et al. *Bioorg Med Chem Lett.* 2010;20:6379.
54. Lo YH, Man CC, et al. *Bioorg Med Chem Lett.* 2004;14:95.
55. Genin MJ, Biles C, Keiser BJ, et al. *J Med Chem.* 2000;43:1034.
56. Guzman-Perez A, Wester RT, et al. *Bioorg Med Chem Lett.* 2001;11:803.
57. Pakal'nis VV, Zerova IV, Yakimovich SI. *Russ J Gen Chem.* 2007;77:1732.
58. Hanif Khan M, Rama NH, Noreen S, Choudhary MI, Jones PG, Iqbal M. *Med Chem Res.* 2012;21:3885.
59. Enthaler S, Weidauer M, Irran E, Epping JD, Kretschmer R, Someya CI. *J Organomet Chem.* 2013;745–746:262.
60. Zelenin KN, Alekseyev VV, Tygsheva AR. *Tetrahedron.* 1995;51:11251.
61. Fustero S, Roman R, Sanz-Cervera JF, et al. *J Org Chem.* 2008;73:3523.
62. Singh SP, Kapoor JK, Kumar D, Threadgill MD. *J Fluorine Chem.* 1997;83:73.
63. Bonacorso HG, Oliveira MR, Costa MB, et al. *Heterocyclic Chem.* 2005;42:631.
64. Irwin JJ, Sterling TT, Mysinger MM, Bolstad ES, Coleman RG. *J Chem Inf Model.* 2012;52:1757.
65. Azimi I, Beilby H, Davis FM, et al. *Mol Oncol.* 2016;10:166.
66. McAndrew D, Grice DM, Peters AA, Davis FM, Stewart T, Rice M, Smart CE, Brown MA, Kenny PA, Roberts-Thomson SJ, Monteith GR. *Mol Cancer Ther.* 2011;10:448.
67. Monteith GR, Bird GS. *Trends Pharmacol Sci.* 2005;26:218.
68. Rice LV, Bax HJ, Russell LJ, et al. *Eur J Pharmacol.* 2013;704:49.
69. Vetter I, Touska F, Hess A, et al. *EMBO J.* 2012;31:3795.
70. Sousa SR, Vetter I, Ragnarsson L, Lewis RJ. *PLoS One.* 2003;8:e59293.